OPTIMIZING PREPARATION CONDITIONS OF ULTRA-LOW-DENSITY FIBERBOARD BY RESPONSE SURFACE METHODOLOGY

Tingjie Chen
E-mail: 83097391@qq.com

Min Niu†
E-mail: 95214960@qq.com

*Yongqun Xie**
College of Material Engineering
Fujian Agriculture and Forestry University
Jinshan, Fuzhou, Fujian Province 350002, People's Republic of China
E-mail: fjxieyq@hotmail.com

(Received January 2015)

Abstract. Preparation conditions of ultra-low-density fiberboard (ULDF) were optimized using the Box–Behnken design and response surface methodology. The effect and interactions of Si-Al molar ratio, additive amount of Si sol, and additive amount of Si-Al compounds on internal bond strength of ULDF were investigated. The regression model for ULDF preparation was significant ($p < 0.0001$), and the Si-Al molar ratio and the additive amount of Si sol had a significant effect on internal bond strength, whereas the additive amount of Si-Al compounds did not. Optimum internal bond strength (12.68 ± 0.35 KPa) was achieved at 500 mL Si-Al compounds with Si-Al molar ratio of 2:1 and 20 mL Si sol. Fourier transform infrared spectra of the ULDF confirmed that some covalent bonds between Si-Al additives and fibers might be formed, and the thermal conductivity, noise reduction coefficient, and contact angle analysis of ULDF further confirmed the validity of the optimal preparation conditions.

Keywords: Internal bond strength, preparation conditions, optimum, response surface methodology, ultra-low-density fiberboard.

INTRODUCTION

Because environmental pollution (Li et al 2011; Pimentel 2003; Trevors 2010) and petroleum-based materials release toxic substances, environmentally compatible materials have recently attracted considerable attention. Ultra-low-density fiberboards (ULDF) are made from plant fibers and are manufactured by a liquid frothing principle (Xie et al 2004, 2008a,b). No heating and pressing or common adhesives such as phenol–formaldehyde resin and urea–formaldehyde resin are used in the preparation process (Niu et al 2014; Xie et al 2011). They are not only economical and safe for human health but can also serve in some applications as substitutes for petroleum-based polymers. They have many excellent properties such as ultra-low densities, low thermal conductivities, and good sound absorption. However, poor mechanical properties that correspond to their ultra-low density have restricted their application (Niu et al 2014; Xie et al 2011). Therefore, interest has increased in modifying the mechanical properties of ULDF with a variety of methods. The mechanical properties of plant-fiber-based materials were improved significantly by inorganic compounds such as SiO_2 (Fu et al 2011; Saka and Ueno 1997), TiO_2 (Mahr et al 2012), and water glass (Lin et al 2013). But, little information is available on the preparation conditions of ULDF for obtaining the desired output characteristics. In addition, previous studies have confirmed that the treatment conditions of inorganic fillers including the additive amount of Si-Al compounds,

* Corresponding author
† SWST member

Si-Al molar ratio, and the additive amount of silicon sol (Si sol) affect the properties of ULDF significantly. For example, Xie and Liu (2012) improved the mechanical properties of ULDF by using the water glass. But the brittleness of materials increased when more water glasses were added. Niu et al (2014) clarified the interactions among the amount of Si-Al compounds, which were generated by aluminum sulfate and sodium silicate and the distribution and fire properties of ULDF from different raw materials. Also, Si sol was added to improve the properties of ULDF in Chen et al (2015). The results indicated that not only the mechanical properties but also the fire properties of ULDF improved. However, the preparation conditions of this process have not been studied further.

To improve the mechanical properties of ULDF, response surface methodology (RSM) was designed to systematically analyze the effects of varieties of inorganic fillers and their interactions. RSM, which is an effective experimental design methodology, has been used widely in scientific research, such as on cellulose nanocrystals (Tang et al 2011), soy flour adhesive for plywood (Chen et al 2013), and wood-based panels (Islam et al 2012; Li et al 2009). Decreasing the number of experimental trials is the main advantage of this methodology. It can not only evaluate multiple parameters and their interactions, but it is also less laborious and time consuming than other approaches required to optimize a process. And it can explore the relationship between several explanatory variable parameters and one or more response variable parameters (Brown and Brown 2012; Mujtaba et al 2014; Sahu et al 2010; Singh et al 2013; Zhong and Wang 2010). Box–Behnken design (BBD), which is one RSM, has only three levels and needs fewer experiments. It is more efficient and easier to arrange and interpret experiments compared with others, and it is widely used by many researchers (Chen et al 2012; Ferreira et al 2007; Tang et al 2011). To the authors' knowledge, few studies have been conducted on optimizing the preparation conditions of ULDF using the RSM approach.

In this study, the Si-Al compounds with different Si-Al molar ratio were prepared and they were then used to make ULDF. To obtain optimal preparation conditions corresponding to good internal bond strength of ULDF, BBD, one of the standard RSM designs, was used to optimize their preparation conditions, including Si-Al molar ratio, additive amount of Si sol, and additive amount of Si-Al compounds.

MATERIALS AND METHODS

Preparation of Si-Al Compound Solution

The Si-Al compound solution with different Si-Al molar ratios (1:1, 2:1, and 3:1) was produced by a reaction between sodium silicate and aluminum sulfate, which were purchased from Tianjin Fu Chen chemical reagents factory (Tianjin, China). The aluminum sulfate solution was first added to a 500-mL trineck round-bottom flask with a magnetic stir bar with vigorous stirring. Then the fixed sodium silicate solution was added to the flask slowly to obtain the Si-Al compound solution.

Preparation of ULDF

ULDFs were manufactured by Kraft pulp (KP, spruce-pine-fir; Tembec Inc., Montreal, Canada) and specimens of $200 \times 200 \times 50\ mm^3$ (L × W × H) were manufactured separately using various parameters in a demonstration line as described by Xie et al (2011), with a target bulk density of 50-60 kg/m^3. The specimen preparation process is described in Fig 1. The additives polyacrylamide resin, alkyl ketene dimer water repellent, chlorinated paraffin fire retardant, and sodium dodecylbenzene sulfonate surfactant were added at 23.8%, 8.4%, 9.5%, and 3.1% of dry fiber weight, respectively.

Internal Bond Strength of ULDF

Internal bond strength of each ULDF was tested in accordance with GB/T 17657 (Standard Press of China 1999). The size of specimens for internal bond strength testing was $50 \times 50 \times 40\ mm^3$

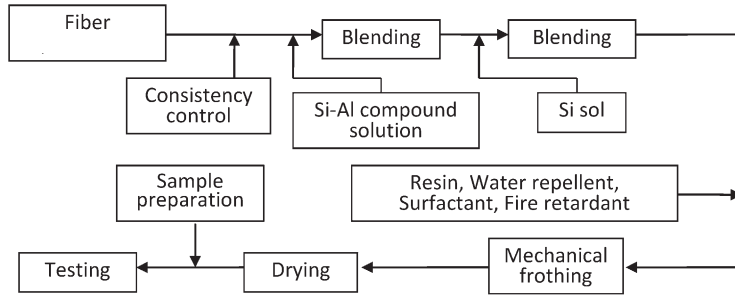

Figure 1. Preparation process of ultra-low-density fiberboards.

(L × W × H). The results were the average of five replicates.

Experimental Design

The Si-Al molar ratio (X_1 = 1:1, 2:1, and 3:1), additive amount of Si sol (purchased from Jiangyin Saiwei technology trade Co., Ltd., Jiangsu, China), (X_2 = 10, 20, and 30 mL), and additive amount of Si-Al compounds (X_3 = 300, 500, and 700 mL) were chosen as variables; and internal bond strength was their function. BBD, which is one of the standard RSM designs, was applied to study the effects of X_1, X_2, and X_3 on Y. The software Design-Expert (Trial Version 8.0.6, Stat-Ease, Minneapolis, MN) was used to analyze data and build the models. The selection range of each variable is shown in Table 1, and the BBD consisted of 17 experiments with 12 experiments organized in a factorial design and another 5 replicated at the central point of the designed model to estimate the pure error sum of squares.

Characterization

The functional groups of ULDF (produced under the control specimen and optimal preparation conditions) were characterized by Fourier transform IR (FTIR) spectroscopy. FTIR analysis of ULDF was performed by means of a Nicolet 380 FTIR spectrometer (Thermo Fisher Scientific Instruments, Fitchburg, WI), using the

Table 1. Box–Behnken design and response to internal bond strength.

	Coded levels			Internal bond strength (MPa)	
Run No.	Si-Al molar ratio (X_1)	Additive amount of Si sol (X_2, mL)	Additive amount of Si-Al compounds (X_3, mL)	Experimental	Predicted
1	−1 (1:1)	−1 (10)	0 (500)	5.70	6.10
2	1 (3:1)	−1	0	8.24	8.06
3	−1	1 (30)	0	7.49	7.67
4	1	1	0	9.23	8.84
5	−1	0 (20)	−1 (300)	7.81	7.30
6	1	0	−1	9.10	9.16
7	−1	0	1 (700)	8.24	8.18
8	1	0	1	8.93	9.45
9	0 (2:1)	−1	−1	7.79	7.91
10	0	1	−1	7.62	7.96
11	0	−1	1	7.70	7.37
12	0	1	1	9.79	9.67
13	0	0	0	12.52	12.68
14	0	0	0	13.03	12.68
15	0	0	0	12.41	12.68
16	0	0	0	12.86	12.68
17	0	0	0	12.59	12.68

KBr pellet method, taking 32 s for each sample with a resolution of 4 cm^{-1}, ranging from 4000 to 400 cm^{-1}.

The thermal conductivity was measured on 100- × 100-mm specimens following GB/T 10294-2008/ISO 8032:1991 (CBMIA 2008), under steady-state conditions using a guarded hot plate apparatus. The noise reduction coefficient (NRC) was determined as the average of sound absorption coefficients measured at 250, 500, 1000, and 2000 Hz frequencies. The sound absorption coefficients for each sample were determined at four frequencies with a diameter of 50 mm and a thickness of 30 mm using the impedance tube method in accordance with GB/T 18696.1-2004 (CAS 2004). The contact angles of ULDF were determined with a static contact angle/interfacial tension meter (JC2000A; Shanghai Zhongchen Digital Technology Co., Ltd, Shanghai, China). The water solution was dropped on the specimens' surface with a special syringe, and static contact angle was measured. The data presented in this study were the average values obtained from at least five measurements.

RESULTS AND DISCUSSIONS

Model Fitting

To determine the effects of the three independent variables, the design matrix and the corresponding results of RSM experiments are shown in Table 1. A regression analysis (Table 2) was carried out to fit mathematical models which represented the internal bond strength of ULDF against the function of the independent variables, and the model for the predicted response Y can be expressed by the following quadratic polynomial equation in terms of coded values:

$$Y = 12.68 + 0.78X_1 + 0.59X_{12} + 0.29X_3 - 0.20X_{11}X_{12} - 0.15X_{11}X_3 + 0.56X_2X_{13} - 2.36X_1^2 - 2.66X_2^2 - 1.80X_3^2 \quad (1)$$

where, Y is the internal bond strength of ULDF and X_1, X_2, and X_3 are the coded variables for Si-Al molar ratio, additive amount of Si sol, and additive amount of Si-Al compounds, respectively.

In general, exploration and optimization of a fitted response surface may produce poor or misleading results unless the model exhibits good fitness (Brown and Brown 2012; Mujtaba et al 2014; Sahu et al 2010; Singh et al 2013; Tang et al 2011; Zhong and Wang 2010). As shown in Table 2, the p-value of the model was less than 0.0001 and the lack-of-fit value was 0.0588. Therefore, it can be concluded that the model's fitness was good. A small value of coefficient of determination (R^2) called a fitness degree, which is a ratio of explained variation to total variation, indicated poor relevance of the dependent variables in the model. The R^2 of this

Table 2. Analysis of variance for regression model for internal bond strength.

Source	Sum of squares	Degrees of freedom	Mean square	F-value	p-Value
Model	84.30	9	9.37	45.87	<0.0001
X_1	4.90	1	4.90	23.99	0.0018
X_2	2.76	1	2.76	13.52	0.0079
X_3	0.68	1	0.68	3.35	0.1098
X_1X_2	0.16	1	0.16	0.78	0.4054
X_1X_3	0.09	1	0.09	0.44	0.5280
X_2X_3	1.28	1	1.28	6.25	0.0409
X_1^2	23.47	1	23.47	114.95	<0.0001
X_2^2	29.70	1	29.70	145.48	<0.0001
X_3^2	13.66	1	13.66	66.89	<0.0001
Residual	1.43	7	0.20		
Lack of fit	1.17	3	0.39	5.95	0.0588
Pure error	0.26	4	0.065	—	—
Correlation total	85.73	16	—	—	—

$p < 0.01$ highly significant; $0.01 < p < 0.05$ significant; $p > 0.05$ insignificant.

model was 0.9833, which implied that 98.33% of the variations could be explained by the fitted model. R^2 was in reasonable agreement with R_{adj}^2. R_{adj}^2 is a correlation degree between observed and predicted value (Chen et al 2012; Ferreira et al 2007; Tang et al 2011). The R_{adj}^2 was 0.9619. This meant that only 3.81% of the total variation was not explained by the model. Therefore, this regression model can explain the true behavior of the system.

Statistical Analyses

The adequacy of the models was further justified through analysis of variance (ANOVA). The ANOVA for the quadratic model for internal bond strength is shown in Table 2. *p*-Values less than 0.05 showed model terms were significant, whereas *p*-values more than 0.05 indicated model terms were insignificant (Amini et al 2008). Therefore, the *F*-value (45.87) and *p*-values (less than 0.0001) implied that this model was significant and only a 0.01% chance could occur because of noise. Conversely, significance of the model was also judged by a lack-of-fit test. As shown in Table 2, *F*-value and *p*-value of the lack of fit were 5.95 and 0.0588, respectively, which implied that it was not significant and a 5.88% chance could occur because of noise. In this case, the Si-Al molar ratio (X_1), additive amount of Si sol (X_2), interaction term (X_2X_3), and three quadratic terms (X_1^2, X_2^2, and X_3^2) affected the internal bond strength of ULDF significantly, whereas additive amount of Si-Al compounds (X_3), X_1X_2, and X_1X_3 were all insignificant to the response. This indicates the significant interaction between the additive amount of Si sol (X_2) and additive amount of Si-Al compounds (X_3). X_1 was the most important factor, and the next most important was the interaction term X_2X_3.

Analysis of Response Surface

To further analyze the effect of the three factors on internal bond strength of ULDF, the three-dimensional (3D) response surface and two-dimensional (2D) contour plots, which were the graphical representations of regression equations, were presented. They provide a method to visualize the relationship between responses and experimental levels of each variable and the type of interactions between two test variables (Zhong and Wang 2010). Here, the relationship between the parameters and response variable was illustrated in a 3D representation of the response surfaces, and 2D contour plots were generated by the model for internal bond strength of ULDF (Fig 2a, b, and c). Combined with the results in Table 2, variables X_1 and X_2 had a significant effect on internal bond strength, whereas the effect of variable X_3 was insignificant. As shown in Fig 2, internal bond strength improved initially and then decreased with increases in all of the variables. The effects of the Si-Al molar ratio (X_1), additive amount of Si sol (X_2), and additive amount of Si-Al compounds (X_3) on internal bond strength had similar trends. But, compared with the Si-Al molar ratio and additive amount of Si sol, internal bond strength was affected only slightly by additive amount of Si-Al compounds. Interaction between Si-Al molar ratio (X_1) and the other two variables (X_2, X_3) did not impact internal bond strength significantly, whereas the interaction between additive amount of Si sol (X_2) and additive amount of Si-Al compounds (X_3) was significant.

Figure 2c shows the 3D response surfaces, the combined effect of additive amount of Si-Al compounds, and additive amount of Si sol for internal bond strength of ULDF at constant Si-Al molar ratio (2:1). Maximum internal bond strength of ULDF (13.03 KPa) was determined at constant additive amount of Si-Al compounds (500 mL).

Optimization of Preparation Conditions

Ranges in optimal preparation conditions for ULDF were obtained using Eq (1) derived from the surface response experiments using Design Expert software (Stat-Ease, Minneapolis, MN). The predicted optimal conditions for preparing ULDF were Si-Al molar ratio 2.2:1, additive amount of Si sol 21.1 mL, and additive amount

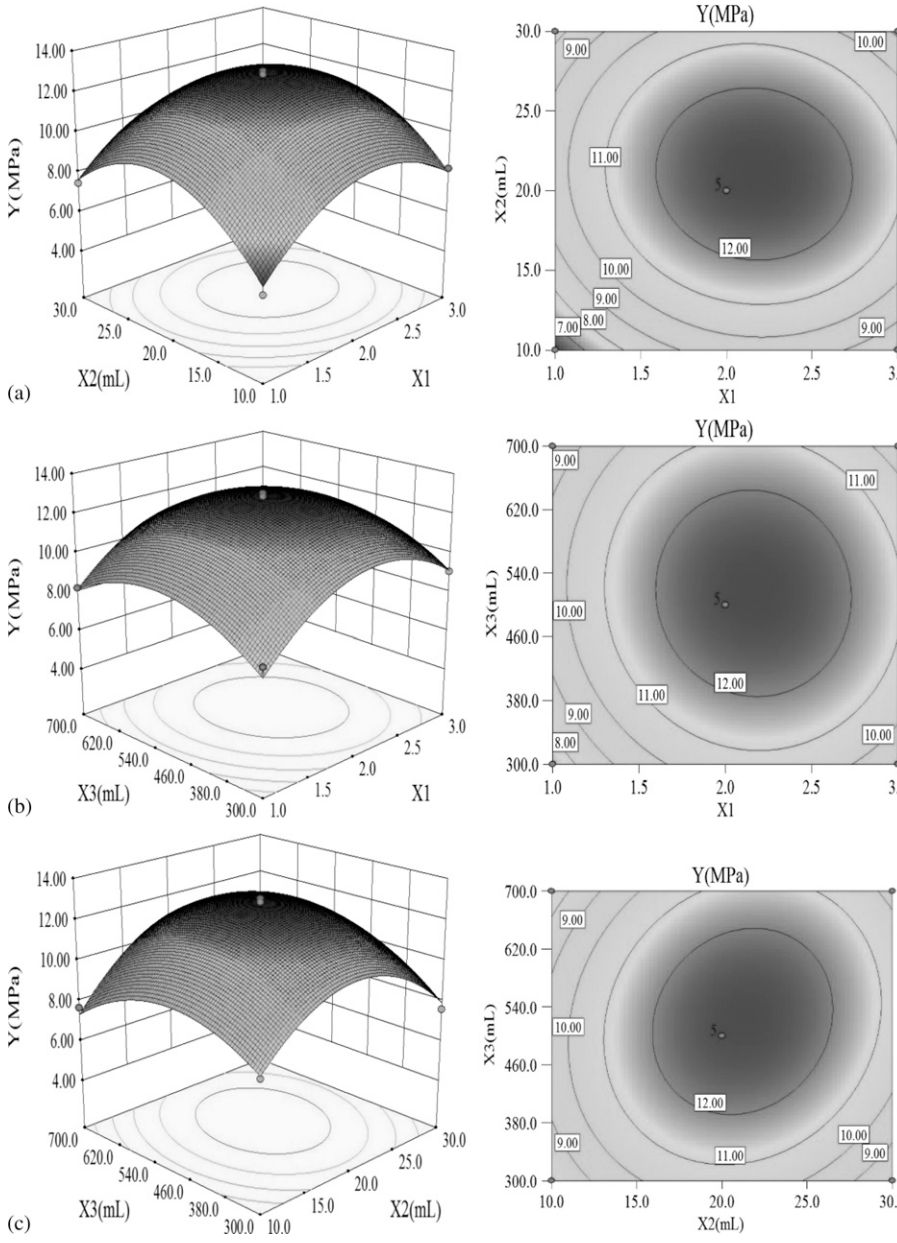

Figure 2. Response surface (left) and contour plots (right) for internal bond strength of ultra-low-density fiberboards (ULDF). (a) Effects of Si-Al molar ratio and additive amount of Si sol on internal bond strength of ULDF. (b) Effects of Si-Al molar ratio and additive amount of Si-Al compounds on internal bond strength of ULDF. (c) Effects of additive amount of Si-Al compounds and additive amount of Si sol on internal bond strength of ULDF.

of Si-Al compounds 518.5 mL. Under these conditions, the model predicts a maximum internal bond strength of 12.79 KPa. Taking practical operating conditions into consideration, some conditions were modified as follows: 500 mL Si-Al compounds with Si-Al molar ratio of 2:1 and 20 mL Si sol. Under these conditions, an average value of 12.68 $\pm$ 0.35 KPa was obtained,

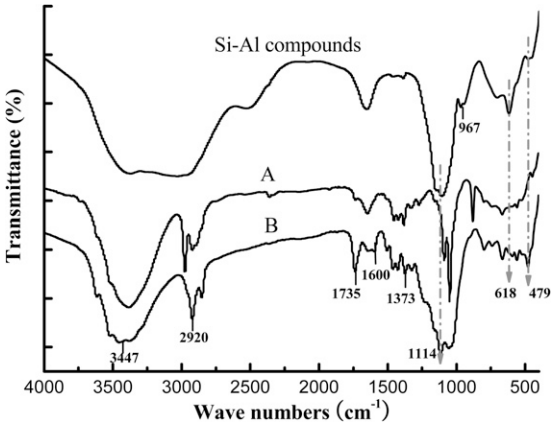

Figure 3. Fourier transform infrared profiles of Si-Al compounds, (a) control specimen and (b) specimen with optimal preparation conditions.

which is close to the model predicted values. This confirms that the model adequately reflects the expected optimization and Eq (1) is satisfactory and accurate.

Fourier Transform IR Analysis

The FTIR spectra of the specimens of ULDF were recorded in the range 4000-400 cm^{-1}. Figure 3 shows the IR spectra of the Si-Al compounds, control specimens (which was a group of specimens without Si-Al compounds and Si sol), and the specimen with optimal preparation conditions. The peaks of Si-Al compounds at 3432, 1108, 967, 618, and 479 cm^{-1} were attributed to the -OH stretching line, Si-O-Si, Si-OH, Al-OH vibrations, and Si-O-Al, respectively. The IR spectra of A and B showed some similar peaks at nearly 3447, 2920, 1600, 1373, and 1034 cm^{-1}, which were assigned to the -OH stretching line, CH_2 stretching vibrations, adsorbed water (which presented abundant hydrophilic hydroxide radical in the cellulose), C-H asymmetric deformations, and C-O stretching vibrations, respectively (Alemdar and Sain 2008; Sun et al 2005). However, the peak of Si-OH (967 cm^{-1}) was disappearing while the Si-Al compounds were added in fiberboard. This was because that the Si-Al compounds were reacted by the fibers. As seen in Fig 3, the additional peaks at about 1114, 618, and 479 cm^{-1} were found in the IR spectra of B compared with A. Among these peaks, because of the similar mass of Al and Si atoms, the broad band in the range of 1200-1000 cm^{-1} usually corresponded to the mixed overlap of Si-O-Si, Al-O-Si, and Si-O-C bonds (He et al 2014). Therefore, the additional peaks at about 1114 cm^{-1} might be attributed to Si-O-Si, Si-O-C, and Si-O-Al. Also, the additional broad peaks at 618 and 479 cm^{-1} were attributed to Al-OH vibrations and Si-O-Al, respectively, which might be explained by the fact that the Si-Al compounds and Si sol had left in ULDF and some covalent bonds had formed between Si-Al inorganic fillers and fibers or other organic fillers.

Physical Properties

The control specimens had a low thermal conductivity of 0.045 W/mK. This was because the porous materials contained a large number of voids. Primary heat transfer is conduction through the still air trapped within the material and natural convection of the air (Xie et al 2011). Thermal conductivity of ULDF with optimal preparation conditions (0.042 W/mK) improved indistinctively (Table 3). The NRC

Table 3. Physical properties of ultra-low-density fiberboards.

Properties		Control specimen	Optimal preparation conditions specimen
Thermal conductivity (W/(m·K))		0.045	0.042
Noise reduction coefficient	250 Hz	0.303	0.611
	500 Hz	0.343	0.827
	1000 Hz	0.969	0.994
	2000 Hz	0.976	0.998
Contact angle (°)		141 ± 0.08	127 ± 0.67

of the ULDF with optimal preparation conditions improved. The NRC of the ULDF with optimal preparation conditions at 250 and 500 Hz were 0.308 and 0.484, respectively, which was higher than control specimens. This meant that the ULDF with optimal preparation conditions could be used as an efficient and practical sound absorber at low frequencies. However, the contact angle of the ULDF with optimal preparation conditions (127°) was lower than the control specimens (141°), which indicated that the waterproof property was decreased because the hydrophilic sodium silicate was added to improve the mechanical properties of ULDF. Taking these factors into consideration, the optimal preparation conditions were valid for preparing ULDF.

CONCLUSIONS

Response surface methodology was used to predict optimal preparation conditions of ULDF. When 500 mL Si-Al compounds with Si-Al molar ratio of 2:1 and 20 mL Si sol were added in preparation process, internal bond strength of 12.68 ± 0.35 KPa was obtained. The regression model for the preparation conditions was satisfactory and accurate, and could be used to navigate the experimental design space. The Si-Al molar ratio and additive amount of Si sol had a significant effect on internal bond strength of ULDF, whereas the additive amount of Si-Al compounds did not. FTIR results revealed that some covalent bonds had formed between Si-Al inorganic fillers and fibers or other organic fillers, and thermal conductivity, NRC, and contact angle analysis of the ULDF further confirmed that the increase in internal bond strength was not at the cost of other properties.

ACKNOWLEDGMENTS

The authors are grateful for the financial support of the National Science and Technology Support Program (2008BADA9B01) and the National Natural Science Foundation of China (NSFC) (30781982).

REFERENCES

Alemdar A, Sain M (2008) Isolation and characterization of nanofibers from agricultural residues: Wheat straw and soy hulls. Biores Technol 99(6):1664-1671.

Amini M, Younesi H, Bahramifar N, Lorestani AA, Ghorbani F, Daneshi A, Sharifzadeh M (2008) Application of response surface methodology for optimization of lead biosorption in an aqueous solution by *Aspergillus niger*. J Hazard Mater 154(1-3):694-702.

Brown JN, Brown RC (2012) Process optimization of an auger pyrolyzer with heat carrier using response surface methodology. Biores Technol 103(1):405-414.

CAS (2004) GB/T 18696.1-2004 Acoustics-determination of sound absorption coefficient and impedance in impedance tubes-part 1: Method using standing wave ratio. Chinese Academy of Science, Standard Press of China, Beijing, China.

CBMIA (2008) GB/T 10294-2008/ISO 8032:1991 Thermal insulation-determination of steady-state thermal resistance and related properties-guarded hot plate apparatus. China Building Material Industry Association, Standard Press of China, Beijing, China.

Chen TJ, Niu M, Wu ZZ, Xie YQ (2015) Effect of silica sol content on thermostability and mechanical properties of ultra-low density fiberboards. BioResources 10(1): 1519-1527.

Chen N, Lin Q, Zeng Q, Rao J (2013) Optimization of preparation conditions of soy flour adhesive for plywood by response surface methodology. Ind Crops Prod 51: 267-273.

Chen W, Wang WP, Zhang HS, Huang Q (2012) Optimization of ultrasonic-assisted extraction of water-soluble polysaccharides from *Boletus edulis* mycelia using response surface methodology. Carbohydr Polym 87(1): 614-619.

Ferreira SLC, Bruns RE, Ferreira HS, Matos GD, David JM, Brandão GC, da Silva EGP, Portugal LA, dos Reis PS, Souza AS, dos Santos WNL (2007) Box-Behnken design: An alternative for the optimization of analytical methods. Anal Chimica Acta 597(2):179-186.

Fu YL, Mo YY, Liu YX, Qiao MJ, Chen WJ (2011) Application of nanometer silicon dioxide in coating and idea of strengthening wood surface properties with nanometer silicon dioxide. J Zhejiang Forestry College 28(4): 644-652 [In Chinese with summary in English].

He F, Chao S, He X, Li M (2014) Inorganic microencapsulated core/shell structure of Al-Si alloy microparticles with silane coupling agent. Ceram Int 40(5): 6865-6874.

Islam MA, Alam MR, Hannan MO (2012) Multiresponse optimization based on statistical response surface methodology and desirability function for the production of particleboard. Compos, Part B Eng 43(3):861-868.

Li P, Huang ZL, Ren H, Liu HX, Wang Q (2011) The evolution of environmental management philosophy under rapid economic development in China. AMBIO 40(1):88-92.

Li X, Li Y, Zhong Z, Wang D, Ratto JA, Sheng K, Sun XS (2009) Mechanical and water soaking properties of medium density fiberboard with wood fiber and soybean protein adhesive. Biores Technol 100(14):3556-3562.

Lin Z, Niu M, Xie YQ (2013) Effects of sodium silicate gel on compressive strength for plant fiber-based foaming composite. Study on preparation and properties of foaming composite. J Fujian College of Forestry 33(4):371-376 [In Chinese with summary in English].

Mahr MS, Hübert T, Schartel B, Bahr H, Sabel M, Militz H (2012) Fire retardancy effects in single and double layered sol-gel derived TiO_2 and SiO_2-wood composites. J Sol-Gel Sci Technol 64(2):452-464.

Mujtaba A, Ali M, Kohli K (2014) Statistical optimization and characterization of pH-independent extended-release drug delivery of cefpodoxime proxetil using Box–Behnken design. Chem Eng Res Des 92(1):156-165.

Niu M, Hagman O, Wang XD, Xie YQ, Karlsson O, Cai LL (2014) Effect of Si-Al compounds on fire properties of ultra-low densities fiberboard. BioResources 9(2): 2415-2430.

Pimentel D (2003) Ethanol fuels: Energy balance, economics, and environmental impacts are negative. Nat Resour Res 12(2):127-134.

Sahu JN, Acharya J, Meikap BC (2010) Optimization of production conditions for activated carbons from Tamarind wood by zinc chloride using response surface methodology. Biores Technol 101(6):1974-1982.

Saka S, Ueno T (1997) Several SiO_2 wood-inorganic composites and their fire-resisting properties. Wood Sci Technol 31(6):457-466.

Singh P, Shera SS, Banik J, Banik RM (2013) Optimization of cultural conditions using response surface methodology versus artificial neural network and modeling of L-glutaminase production by *Bacillus cereus* MTCC 1305. Biores Technol 137:261-269.

Standard Press of China (1999) GB/T 17657. Test methods for evaluating the properties of wood-based panels and surface decorated wood-based panels. Standard Press of China, Beijing, China.

Sun X, Xu F, Sun R, Fowler P, Baird M (2005) Characteristics of degraded cellulose obtained from steam-exploded wheat straw. Carbohyd Res 340(1):97-106.

Tang LR, Huang B, Ou W, Chen XR, Chen YD (2011) Manufacture of cellulose nanocrystals by cation exchange resin-catalyzed hydrolysis of cellulose. Biores Technol 102(23):10973-10977.

Trevors JT (2010) What is a global environmental pollution problem. Water Air Soil Pollut 1(4):1-2.

Xie YQ, Chen Y, Wei QH, Zhang DZ (2008a) Study on forming a truss-like reticular structure made from nature fiber under the effect of liquid frothing. J Fujian College of Forestry 28(3):203-207 [In Chinese with summary in English].

Xie YQ, Chen Y, Zhang BG (2004) Study on a foamed material from plant fibers. China Wood Industry 18(2): 30-32 [In Chinese with summary in English].

Xie YQ, Liu JH (2012) Reinforcement of plant fiber-based ultra low density material with sodium silicate. J Beijing Forestry University 34(1):4-5 [In Chinese with summary in English].

Xie YQ, Tong QJ, Chen Y (2008b) Construction mechanism of reticular structure of plant fiber. J Korea Furniture Soc 19(2):106-110 [In Chinese with summary in English].

Xie YQ, Tong QJ, Chen Y (2011) Manufacture and properties of a novel ultra-low density fiberboard. BioResources 6(4):4055-4066.

Zhong K, Wang Q (2010) Optimization of ultrasonic extraction of polysaccharides from dried longan pulp using response surface methodology. Carbohydr Polym 80(1):19-25.